

Style Definition: Default Paragraph Font

# Investigating the vertical extent of the 2023 summer Canadian wildfire impacts with satellite observations

Selena Zhang<sup>1</sup>, Susan Solomon<sup>1</sup>, Chris D. Boone<sup>2</sup>, Ghassan Taha<sup>3,4</sup>

<sup>1</sup>Department of Earth, Atmospheric, and Planetary Sciences, Massachusetts Institute of Technology, Cambridge, MA 02139, USA

<sup>2</sup>Department of Chemistry, University of Waterloo, Waterloo, Ontario N2L 3G1, Canada

<sup>3</sup>Morgan State University, Baltimore, MD 21251, USA

<sup>4</sup>NASA Goddard Space Flight Center, Greenbelt, MD 20771, USA

10 Correspondence to: Selena Zhang (selenaxz@mit.edu)

**Abstract.** Pyrocumulonimbus clouds (pyroCbs) generated by intense wildfires can serve as a direct pathway for the injection of aerosols and gaseous pollutants into the lower stratosphere, resulting in significant chemical, radiative, and dynamical changes. Canada experienced an extremely severe wildfire season in 2023, with a total area burned that substantially exceeded those of previous events known to have impacted the stratosphere (such as the 2020 Australian fires). This season also had record-high pyroCb activity, which raises the question of whether the 2023 Canadian event resulted in significant stratospheric perturbations. Here, we investigate this anomalous wildfire season using retrievals from [multiple](#) satellite instruments, ACE-FTS (Atmospheric Chemistry Experiment – Fourier Transform Spectrometer), OMPS LP (Ozone Mapping and Profile Suite Limb Profiler), [and](#) [MLS \(Microwave Limb Sounder\)](#) to determine the vertical extents of the wildfire smoke along with chemical signatures of biomass burning. These data show that smoke primarily reached the upper troposphere [and](#) only a nominal amount managed to penetrate the tropopause. Only [a few](#) ACE-FTS [occultations](#) captured elevated [abundances](#) of biomass burning products in the [lowermost](#) stratosphere. OMPS LP aerosol measurements [also](#) indicate that any smoke that made it past the tropopause did not last long [enough or reach high](#) enough to significantly perturb stratospheric composition. While this work focuses on Canadian wildfires given the extensive burned area, pyroCbs at other longitudes (e.g. Siberia) are also captured in the compositional analysis. These results highlight that despite the formation of many pyroCbs in major wildfires, those capable of penetrating the tropopause are extremely rare; this in turn means that even a massive area burned is not necessarily an indicator of stratospheric effects.

Deleted: two

Deleted: ) and

Deleted: but

Deleted: one

Deleted: occultation

Deleted: concentrations

Deleted: lower

Deleted: on July 30<sup>th</sup>, and back and forward trajectories place the source fire in the Yukon. However,...

## 1 Introduction

In 2023, a record-breaking fire season burned over [1.5](#) million [hectares](#) in Canada, [over seven](#) times the 1983 – 2022 annual average burned area of [2.1](#) million [hectares](#) (Canadian Interagency Forest Fire Centre Inc., <https://ciffc.net/statistics/>). These events follow a trend of increasingly extensive and destructive wildfires, often referred to as megafires, that are projected to become more frequent under a changing climate (Di Virgilio et al., 2019; Williams et al., 2019; Pausas and Keeley, 2021). In

Deleted: 45

Deleted: acres

Deleted: almost ten

Deleted: 5.

Deleted: acres

addition to the well-studied impacts of megafires on air quality and tropospheric composition, a number of events have also injected wildfire smoke into the stratosphere via deep convective events known as pyrocumulonimbus clouds (pyroCbs) (Fromm et al., 2010; Fromm et al., 2019; Fromm et al., 2022).

50 PyroCbs are towering thunderstorms triggered by intense surface fire activity that also require specific meteorological conditions for development (including very dry surface conditions and high moisture and instability in the mid-troposphere, see Peterson et al., 2017). [Strong evidence has been presented to show that past wildfire events injected significant amounts of smoke above the tropopause and that smoke-charged vortices may also self-loft \(Khaykin et al., 2020; Renard et al., 2020; Lestrelin et al., 2021; Sellitto et al., 2023\)](#). Perhaps the most notable example of these effects is the 2019 – 2020 Australian  
55 New Year Super Outbreak (ANYSO) event that injected up to 1.1 Tg of smoke into the stratosphere (Peterson et al., 2021). ANYSO, which was part of the Australian “Black Summer” bushfire season where [around 5.8 million hectares](#) burned, has been linked to stratospheric ozone depletion and numerous climate impacts (Boer et al., 2020; Kablick et al., 2020; Rieger et al., 2021; Bernath et al., 2022; Solomon et al., 2023). While the Black Summer fires raged for about seven months, nearly all the stratospheric input occurred on just a few days; December 29-31, 2019 and January 4, 2020. (Davey and Sarre, 2020; Khaykin et al., 2020; Peterson et al., 2021). [Stratospheric perturbations also occurred as a result of the 2017 Pacific Northwest Event \(PNE\) in British Columbia, when on August 12, 2017, pyroCbs injected an estimated 0.3 Tg of aerosols into the stratosphere \(Peterson et al., 2018; Torres et al., 2020\). For context compared to 2023, the 2017 Canadian wildfires burned a total of 3.5 million hectares, with over 1.2 million hectares burned in British Columbia \(Government of British Columbia, <https://www2.gov.bc.ca/>\).](#)

65 Given the outsized area burned in the 2023 Canadian wildfires, significant stratospheric impacts perhaps as in the PNE or ANYSO events might be expected. It has been reported that at least 135 pyroCbs occurred in Canada between May and August 2023, a record-high amount further suggesting the possibility of substantial perturbations to stratospheric composition (Smith, 2023). Recent research has investigated the tropospheric impacts of the 2023 fires, identifying record-  
70 high particulate matter emissions with implications for air quality and human health, but the vertical extent of these impacts and whether smoke entered the stratosphere has not yet been reported (Thurston et al., 2023; Wang et al., 2023).

The Atmospheric Chemistry Experiment – Fourier Transform Spectrometer (ACE-FTS) is a satellite instrument that detects a number of species including multiple biomass burning tracers with high sensitivity and precision (Sect. 2.1). Here, we use  
75 data from ACE as well as aerosol extinction data from the Ozone Mapping and Profiler Suite Limb Profiler (OMPS LP), described in Sect. 2.2, to investigate whether the 2023 Canadian wildfires perturbed stratospheric composition. [MLS carbon monoxide data is also analyzed.](#)

**Deleted:** Some pyroCbs can perturb stratospheric composition in a manner similar to volcanoes.Strong evidence

**Deleted:** Khaykin et al., 2020;

**Deleted:** over 14

**Deleted:** acres

**Deleted:**

**Deleted:**

**Deleted:** 8.6

**Deleted:** acres

**Deleted:** 3

**Deleted:** acres

**Deleted:** NASA EarthData, <https://www.earthdata.nasa.gov/>.

**Deleted:** These data products, combined with back and forward trajectories from the NOAA Hybrid Single-Particle Lagrangian Integrated Trajectory (HYSPPLIT) model as detailed in Sect. 2.3, are then used to connect chemical signatures of stratospheric smoke to potential source fires.MLS carbon monoxide data is also

## 95 2 Data and methods

### 2.1 ACE-FTS and MLS data

ACE-FTS aboard the Canadian ACE/SCISAT-1 platform is a solar occultation instrument that collects up to 30 daily atmospheric absorption measurements at sunrise and sunset using the Sun as a light source (Bernath, 2005; Bernath, 2017). The infrared Fourier transform spectrometer measures over a wide spectral range (750 to 4400  $\text{cm}^{-1}$ ) with a high resolution of 0.02  $\text{cm}^{-1}$  and signal-to-noise ratio ranging between 100:1 and 400:1 (Buijs et al., 2013). The ACE-FTS processing version 5.2 provides vertical volume mixing ratio (VMR) profiles for 46 molecules and 24 isotopologues including characteristic biomass burning indicator molecules such as carbon monoxide (CO), hydrogen cyanide (HCN), acetonitrile ( $\text{CH}_3\text{CN}$ ), and ethane ( $\text{C}_2\text{H}_6$ ) (Boone et al., 2023). A pair of filtered imagers also measures atmospheric extinction at two wavelengths: visible (VIS, 527.11 nm) and near-infrared (NIR, 1020.55 nm). The NIR imager is less likely to become saturated in cases of strong aerosol extinction and was thus used in this analysis for detection of aerosol loads (Vanhellemont et al., 2008; Boone et al., 2020). Temperature profiles are also collected with every occultation and were used to calculate tropopause heights (Sect. 2.3). Data from ACE are available at [https://database.scisat.ca/level2/ace\\_v5.2/](https://database.scisat.ca/level2/ace_v5.2/) starting from 2004.

Given the limited data coverage of ACE, we also analyze carbon monoxide data from the Microwave Limb Sounder (MLS) aboard the NASA Aura satellite (Waters et al., 2006) given its higher spatial coverage. The MLS instrument has seven radiometers that measure microwave thermal emissions between 118 GHz and 2.5 THz from the limb of the atmosphere to determine vertical profiles of atmospheric constituents. This instrument has a much higher spatial coverage than ACE, but the use of microwave spectroscopy provides data with a lower signal-to-noise ratio on individual soundings and a more limited vertical range. For example, the CO data product is recommended for scientific use between 215 – 0.001 hPa, while the HCN and  $\text{CH}_3\text{CN}$  valid ranges are even smaller at 21 – 0.1 hPa and 46 – 1.0 hPa respectively (Livesey et al., 2022). Since we are interested in the vertical profiles of biomass burning products, MLS is not as useful as ACE for our analysis given the lack of reliable data at our pressure range of interest in the lowermost stratosphere and its transition to the tropopause and upper troposphere. However, carbon monoxide data from MLS in the lower stratosphere is still useful as complementary data since strong signals from large perturbations would be clearly detected (Fig. S1). Additionally, comparison of ACE and MLS profiles in our latitude range of interest supports our conclusions from ACE data despite more limited coverage (Fig. S2). Data from MLS are available at [https://disc.gsfc.nasa.gov/datasets/ML2CO\\_NRT\\_005/summary](https://disc.gsfc.nasa.gov/datasets/ML2CO_NRT_005/summary), starting from 2004.

### 2.2 OMPS LP aerosol data

OMPS LP on the Suomi NPP satellite is a limb profiler that measures scattered UV, visible, and near-IR radiation. Aerosol extinction coefficients are retrieved for six wavelengths (510, 600, 675, 745, 849, and 997 nm) with the V2.1 algorithm (Taha et al., 2021). OMPS LP measures along Earth's limb with three parallel vertical slits, one central slit that views along

Deleted: measurement

Deleted: as defined by the WMO: the lowest altitude at which the lapse rate decreases below(Sect.

Deleted:  $\text{K km}^{-1}$  (WMO, 1957

Formatted: Font color: Auto

Formatted: Font color: Auto

Deleted: compare its CO measurements to

Moved down [1]: S1).

Deleted: Thus,

Deleted: compare ACE and MLS CO

Deleted: to validate the robustness

Deleted: our results (Fig.

Deleted: We find through this comparison that the volume mixing ratios from the two instruments are within reasonable agreement of each other, but...

Formatted: Font color: Auto

Deleted: , particularly for individual soundings,

Moved (insertion) [1]

Deleted: .

Deleted:

Deleted: ¶

145 the nadir track and two side slits viewing with a cross-track separation of 250 km at the tangent point allowing for near-  
global daily coverage. The 745 nm channel was used in this analysis given its high sensitivity to aerosol loading and low  
bias, and aerosol extinction is analyzed as an indicator for aerosol abundance. A cloud detection algorithm detects the  
150 highest cloud altitude and flags all aerosol extinction measurements below the peak cloud level, allowing for a cloud-filtered  
data product (Chen, 2016). The retrieved aerosol-to-molecular extinction ratio analyzed in this work is analogous to an  
aerosol mixing ratio, see Loughman et al., 2018 and Taha et al., 2022 for a detailed account of the retrieval algorithm and  
previous data applications. Data from OMPS is available at [https://disc.gsfc.nasa.gov/datasets/OMPS\\_NPP\\_LP\\_L2\\_AER\\_DAILY\\_2/summary](https://disc.gsfc.nasa.gov/datasets/OMPS_NPP_LP_L2_AER_DAILY_2/summary).

### 2.3 Tropopause height calculation

155 Determination of stratospheric entry depends on the definition of tropopause height. Given the high variability of tropopause  
heights, using data that is specific to the time and location of the VMR and aerosol extinction measurements of interest is  
important. Concurrent temperature profiles are retrieved alongside VMR profiles from ACE; specifically, ACE temperature  
profiles are determined from 18 km upwards from data retrievals while temperatures and pressures below 18 km are fixed to  
data from the Canadian Meteorological Centre weather model (Sica et al., 2008). Therefore, a temperature-based tropopause  
definition, the WMO lapse rate tropopause, was used in this study (WMO, 1957).

160 In practice, the lapse rate tropopause was calculated by first determining the lapse rate of the ACE temperature profile at  
every vertical level, and interpolating to determine slope values between the 1 km vertical intervals. Every vertical level  
where the lapse rate reached  $-2 \text{ K km}^{-1}$  was marked, and the lowest level at which the lapse rate passed this threshold was  
determined to be the tropopause altitude. For temperature profiles that exhibit a double tropopause, this method provides the  
lower tropopause altitude (Peevey et al., 2012; Homeyer et al., 2014).

## 165 3 Results and discussion

### 3.1 Chemical signatures for biomass burning

The tropopause acts as a strong barrier to troposphere-to-stratosphere transport, and the high vertical resolution of ACE is  
useful in determining whether smoke entered the stratosphere. Individual occultation measurements from ACE provide  
170 simultaneous constituent volume mixing ratio (VMR) and temperature profiles where biomass burning product VMRs can  
be compared against self-consistent tropopause heights as measured on the same occultation and in broader averages. HCN  
is a robust wildfire tracer for the Northern hemisphere because its primary source is biomass burning (Li et al., 2000; Roberts  
et al., 2020). In contrast, other tracers like CO and ethane are emitted in large amounts by both wildfires and anthropogenic  
sources such as transportation and industry (Xiao et al., 2004), complicating source attribution for those compounds.

**Deleted:** . Data from OMPS is available at [https://disc.gsfc.nasa.gov/datasets/OMPS\\_NPP\\_LP\\_L2\\_AER\\_DAILY\\_2/summary](https://disc.gsfc.nasa.gov/datasets/OMPS_NPP_LP_L2_AER_DAILY_2/summary) starting from 2012....

**Deleted:** 2.3 NOAA HYSPLIT  
NOAA HYSPLIT is a trajectory model developed by the National Oceanic and Atmospheric Administration Air Resources Laboratory (NOAA ARL) that is used to simulate atmospheric transport, dispersion, and deposition of pollutants (Stein et al., 2015). The model is compatible with numerous meteorological datasets and in this study was run on reanalysis data from the National Centers for Environmental Prediction (NCEP) Global Forecast System (GFS) 0.25 degree grid. Trajectories are initialized from an air parcel defined by its altitude, latitude, longitude, and time and run for a prescribed time period. The model is available at <https://www.ready.noaa.gov/HYSPLIT.php>.

**Deleted:**

**Deleted:** concentrations

**Deleted:** ,

Additionally, wildfires are not the only source of particles in the stratosphere, especially in the recent context of the Hunga Tonga–Hunga Ha’apai and Shiveluch eruptions in the last couple of years. This is why we focus on chemical data from ACE–FTS in addition to aerosol data to be able to confidently attribute wildfires as the source.

We first investigate average monthly HCN volume mixing ratio (VMR) profiles. Some individual occultations do not extend into the troposphere, so monthly averages in absolute altitude capture the maximum amount of data to compare 2023 with the rest of the ACE–FTS measurement period (2004 to 2022). A tropopause-relative framework is used in Sect. 3.2 to detect individual measurements of stratospheric smoke. Chemical anomalies detected in the region from 40° to 70° that are likely associated with wildfires, also reflect other active burning regions such as Siberia (MODIS, <https://modis.gsfc.nasa.gov/>). Figure 1 suggests an enhancement of HCN in the upper troposphere and lowermost stratosphere (UTLS) between June and September 2023 relative to preceding years, with the monthly average tropopause heights calculated from ACE–FTS temperature profiles representing a rough delineation between the troposphere and stratosphere. On average, enhancements do not extend more than a couple kilometers above the tropopause. Similar results can be seen for single profiles (Fig. S3).

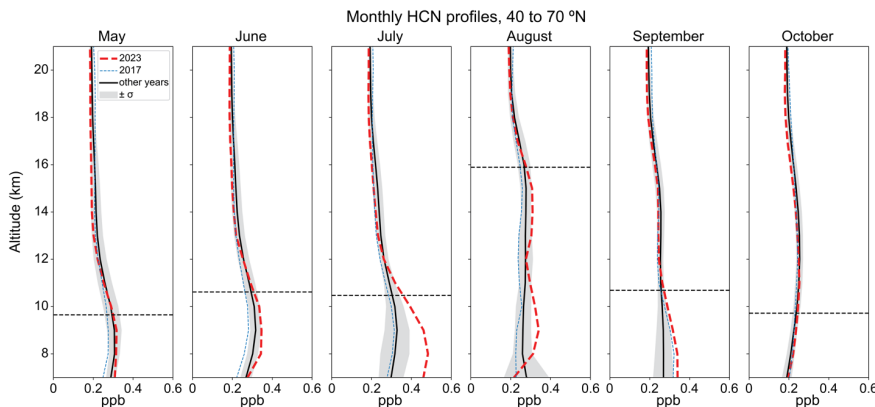


Figure 1: Monthly average HCN profiles from 40 to 70° N measured by ACE–FTS. The red curves show monthly averages in 2023, and the black curves show monthly averages from 2004–2022 with the grey shaded area representing  $\pm$  one standard deviation from the 2004–2022 average. The blue dashed line indicates 2017 averages as it was an anomalous year with the PNE. The monthly average lapse rate tropopause altitudes calculated for 2023 are plotted as horizontal dashed lines for reference.

ACE/SCI–SAT1 takes a very limited number of measurements over our latitude range of interest during August as seen in Table S1; only 20 measurements were taken in August 2023, and all on the first couple of days of the month and between 40 and 45° N. This may explain the unusually high tropopause altitude for this month as tropopause altitudes are higher closer to the equator and previous studies with ACE in August also report a higher tropopause height (Doeringer et al., 2012). Additionally, a low number of measurements are likely more susceptible to transient meteorological influences such as the

- Deleted: compare
- Deleted: in 2023 to
- Deleted: across
- Deleted: ) in the
- Deleted: N to identify when anomalous concentrations occur
- Deleted: very
- Deleted: . Chemical signatures detected in this latitude range
- Deleted: wildfire
- Deleted: <https://modis.gsfc.nasa.gov/>.
- Deleted: what is typical in
- Deleted: But on
- Deleted: significant
- Deleted: few
- Deleted: S2

- Deleted: <object>
- Deleted: 2017 is differentiated by the
- Deleted: approximate
- Deleted: ¶
- Deleted: (
- Deleted: ); in 2023,
- Deleted: only
- Deleted:
- Deleted: such limited temporal and spatial scales
- Deleted: more subject
- Deleted: influence of external processes

Asian monsoon (Basha et al., 2020). [ERA5 reanalysis data collocated at ACE measurement points and times for August yield a similarly high average tropopause height of 14.6 km \(Herschbach et al., 2023\).](#)

The range given by the standard deviation of ACE data from 2004 to 2022 indicates that there were likely other wildfire years that also produced high HCN [mixing ratios](#) from June to September, but 2023 is on the upper end of this spread from about 8 to 11 km. July 2023 in particular has noticeably higher [abundances](#) compared to the range of previous years.

Although this HCN enhancement is indicative of wildfire smoke reaching the upper troposphere, the occurrence of stratospheric injection is less clear given the variability of tropopause heights and the limited number of observations, particularly in August (see Table S1). [This limited coverage and amount of August data ACE is supplemented by the higher coverage of OMPS as shown in the following section and MLS in the supplemental information.](#)

The average July 2023 profiles of other biomass burning markers such as CO, CH<sub>3</sub>OH, HCOOH, and C<sub>2</sub>H<sub>6</sub>, also exhibit elevated [VMRs](#) in the upper troposphere but not significantly so in the lowermost stratosphere (Fig. 2).

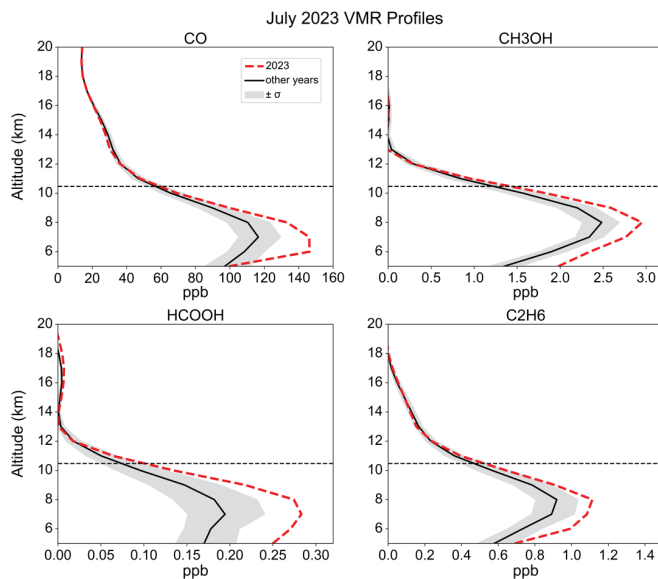


Figure 2: Average July 2023 VMR profiles for additional biomass burning tracers: CO, CH<sub>3</sub>OH, HCOOH, and C<sub>2</sub>H<sub>6</sub>, plotted against 2004–2022 July averages over 40° N to 70° N. The grey shaded area represents ± one standard deviation based on 2004–2022 data.

Deleted: concentrations

Deleted: concentrations

Formatted: Space After: 10 pt

Deleted: concentrations

Deleted: . These data provide strong evidence for the vertical transport of wildfire smoke to the upper troposphere due to high pyroCb activity during the summer wildfire season. However, significant stratospheric penetration is not observed...

Deleted: <object>

These data provide strong evidence for the vertical transport of wildfire smoke to the upper troposphere due to high pyroCb activity during the summer wildfire season, which can influence upper tropospheric composition and chemistry (e.g. ozone production). However, significant stratospheric penetration is not observed in the averages.

### 3.2 Stratospheric smoke signatures

Inspection of every individual occultation measured by ACE-FTS over the 40 to 70° N latitude band in the 2023 burning season revealed a few occultations indicative of stratospheric smoke, exhibited by enhanced chemical signatures and aerosol extinction above the tropopause. These measurements offer evidence of a small amount of smoke in the lowermost stratosphere. The July occultations that exhibit multiple biomass burning products and aerosol extinction measured in the stratosphere are shown in Fig. 3, and similar profiles for other months are shown in Figure S5.

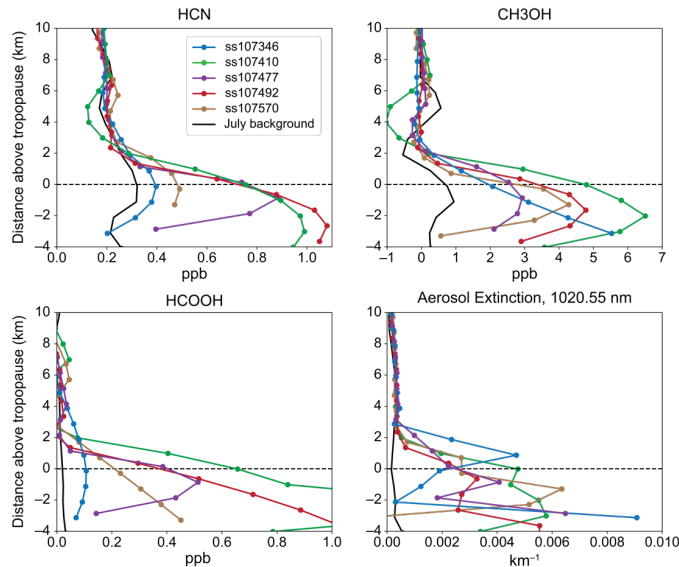


Figure 3: Tropopause-relative profiles for July 2023 occultations that exhibit enhanced wildfire product VMRs and aerosol extinction in the lower stratosphere. A background profile with no smoke from a similar location in July 2023, ss107249, is plotted for reference.

Elevated VMRs of multiple biomass burning products measured above the tropopause in these data offer evidence for a nominal amount of wildfire smoke in the stratosphere. To further validate this conclusion, the ACE infrared absorption

Deleted: 3.2 Occultation ss107570

Deleted: July

Deleted: one occultation measurement

Deleted: injection because it

Deleted: both clear

Deleted: (Fig. S2). This measurement, ss107570, was taken on July 30<sup>th</sup> 04:26 UTC over 49.14° N, 132.10° W off the coast...

Deleted: British Columbia, and

Deleted: profiles

Deleted: . The temperature profile retrieved with this occultation indicates a lapse rate tropopause at around 10 km...

Deleted: <object>

Deleted: Biomass burning

Deleted: VMR

Deleted: profiles for occultation ss107570, which all exhibit enhanced concentrations in the lower stratosphere. The July

Deleted: The July 2004 – 2022 averaged profiles of the gaseous products are...

Deleted: with the altitude adjusted to distance above tropopause height...

Deleted: concentrations

Deleted: ss107570

Deleted: entering

Deleted: in late July.

spectra were also analyzed for features characteristic of wildfire smoke, as in Boone et al. (2020). Carbonaceous aerosols typically exhibit C–H, O–H, and C–C features associated with alkanes and oxygenated organics, and these are indeed present for these occultations, for example as shown in the IR spectrum in Fig. 4 (Zhong and Jang, 2014; Boone et al. 2020; Bernath, 2020). The O–H stretch is commonly seen in smoke particles and indicates that they are oxygenated (Boone et al., 2020). The C=O stretch, which is also associated with oxygenated smoke particles and identified using a feature around 1750 cm<sup>-1</sup>, cannot be seen because that region is saturated at lower altitudes by strong absorption of water vapor in the same spectral region.

Deleted: spectrum was

Deleted: on this occultation

Formatted: Font color: Text 1

Formatted: Font color: Red

Deleted: .

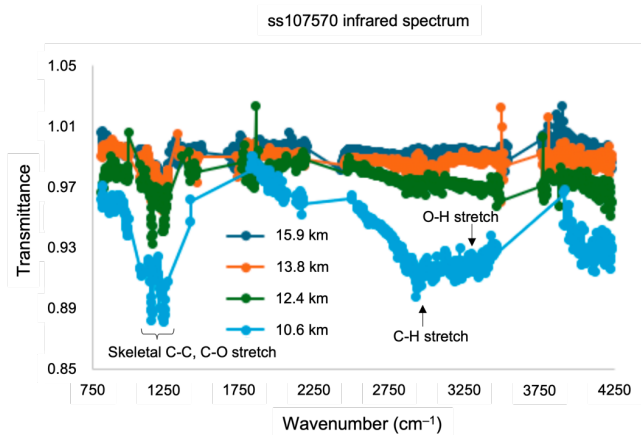


Figure 4: Residual IR spectrum for ss107570 measured at multiple tangent heights. The highlighted features at 10.6 km are indicative of smoke. At higher altitudes, the spectrum becomes plume-free and there are no longer indicators of smoke.

Deleted: <object>

Deleted: a

Deleted: height of 10.6 km.

Moved (insertion) [2]

Given the extent of Canada’s wildfire season, using fire databases to identify potential source fires is non-trivial given the large number of events in 2023 with extensive burned areas (Canadian Interagency Forest Fire Centre Inc, <https://ciffc.net/national>). Thus, more targeted methods for identifying pyroCb-specific fires are a more promising approach for this analysis. Cross-referencing with an online crowdsourced pyroCb database (<https://groups.io/g/pyrocb>) suggests a few pyroCb events with brightness temperatures below -55 °C. A cold cloud top of this magnitude is indicative of deep overshooting convection that may penetrate the tropopause and enter the stratosphere (Romps et al., 2009). It is therefore plausible that these pyroCbs injected smoke into the stratosphere.

Moved (insertion) [3]

Back trajectories initialized from ACE stratospheric smoke measurements on NOAA HYSPLIT with GDAS 1<sup>o</sup> meteorological data do not directly intercept any of these reported pyroCbs, but this is not surprising given the limited spatial coverage of ACE. Trajectories initialized from two occultations, ss107346 and ss107570, pass within tens of



kilometers and a few hours of reported pyroCbs and are shown in Fig. S6. Despite the lack of direct detection, chemical signatures of smoke after dispersion in the lower stratosphere are clearly measured and show the limited vertical range of wildfire influence in the stratosphere: within 2 km above the tropopause.

### 3.3 OMPS LP Aerosol data

Aerosol extinction data from OMPS LP also indicate a minor increase in aerosol burden in the lower stratosphere averaged between 11.5 and 16.5 km, in late July 2023 (Fig. 5). However, this increase above background levels is both small in magnitude and short-lived, which indicates that not enough smoke was injected into the stratosphere to significantly impact extinction measurements. Throughout the entire wildfire season, there are no significant aerosol extinction signals at this altitude range that would suggest deep convective wildfire events. This validates our general finding that very little smoke managed to make it well above the tropopause despite high pyroCb activity, suggesting that the many convective events that occurred were mostly limited to the upper troposphere. There is a constant background level of aerosols above 60° N, but this feature is present from the beginning of 2023 and therefore is not linked to the 2023 Canadian wildfire events but rather other aerosol sources such as volcanic eruptions.

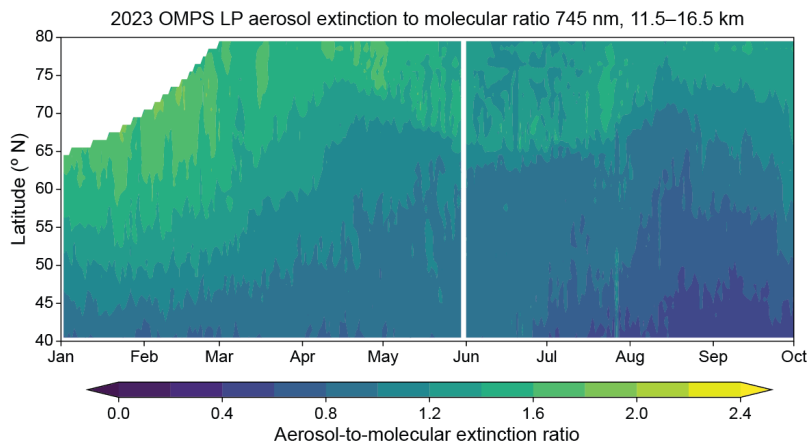


Figure 5: Zonally averaged daily OMPS extinction to molecular ratio between 11.5 and 16.5 km, 40 to 80° N. This represents the evolution of average aerosol load in the lower stratosphere during the 2023 summer wildfires.

The altitude range between 10.5 and 11.5 km contains either tropospheric or stratospheric air depending on the latitude and time of year, and analysis of OMPS data at this altitude reveals substantial average aerosol loading in the region around the tropopause in 2023 (Fig. 8, middle panel). This suggests that the many pyroCbs of the 2023 wildfire season alongside other

Deleted: small

Deleted: lowermost

Deleted: minor

Deleted: 60°

Deleted: <object>

Deleted:

Deleted: S5

aerosol sources managed to inject particles right around the tropopause. However, the [significantly lower aerosol extinction](#) signal past 11.5 km as seen in Fig. 5 and Fig. S7 constrains these inputs to the region at or just above the tropopause as opposed to higher in the stratosphere where more impacts would be realized.

### 3.4 Comparison to Pacific Northwest Event

To contextualize the [2023 Canadian events](#), we compare its ACE-FTS profiles with measurements of the 2017 PNE which also occurred in western Canada during the summer. Analysis of this event was previously reported in Boone et al. 2020, with the occultation sr75758 probing the plume a few weeks after initial stratospheric injection. Figure 6 shows a substantial difference in [smoke](#) altitude, with the 2017 PNE [leading to chemical signatures of biomass burning products measured above 20 km](#) compared to the [much lower vertical extent](#) of the 2023 [fires](#).

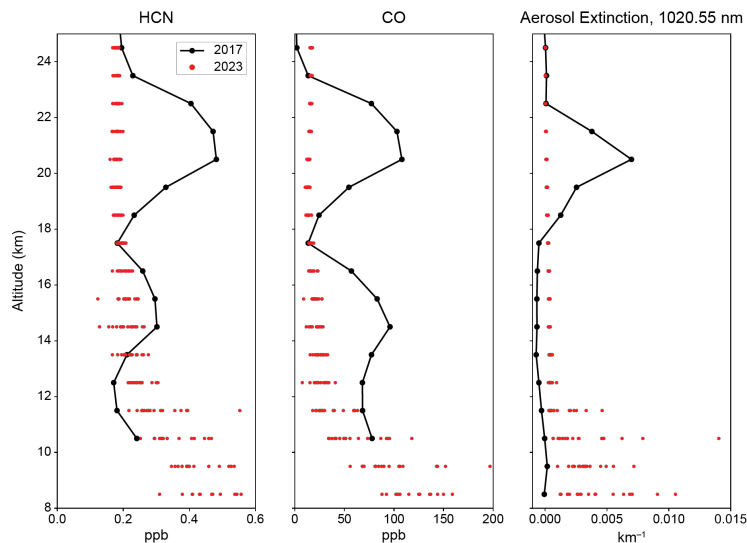


**Figure 6:** Biomass burning product VMR and aerosol extinction profiles for occultation sr75758 (black) associated with the 2017 Pacific Northwest Event (Boone et al., 2020). Profiles from the [2023 Canadian wildfires that exhibited stratospheric penetration](#) are shown in red for comparison.

The top panel of Fig. 7 also shows with OMPS data that 2017 featured a much larger injection of aerosols between 11.5 and 16.5 km relative to 2023, where there is no evident increase in average stratospheric aerosol extinction throughout the entire summer. Similarly, the bottom panel of Fig. 7 contrasted to Fig. 5 shows that the magnitude and duration of stratospheric perturbation from the PNE was much more substantial than that of any pyroCb activity from 2023. Since ACE-FTS

**Deleted:** significant decrease in

**Moved up [2]:** Given the extent of Canada's wildfire season, using fire databases to identify potential source fires is non-trivial given the large number of events in 2023 with extensive burned areas (Canadian Interagency Forest Fire Centre Inc, <https://ciffc.net/national>). Thus, more targeted methods for identifying pyroCb-specific fires are a more promising approach for this analysis. Cross-referencing with an online crowdsourced

**Moved up [3]:** the stratosphere (Romps et al., 2009).

**Deleted: Trajectory analysis** ¶  
The preceding data provide evidence for stratospheric entry of smoke around the location and date of ss107570. Back trajectory analyses enable the identification of potential source fires that generated a pyroCb capable of direct stratospheric injection. 72 hour trajectories ending at the point of measurement were run on NOAA HYSPLIT and are shown in Fig. 6, with possible source fire locations concentrated in the Yukon and Northwest Territories. ¶  
**<object>**Figure 6: 72 hour HYSPLIT back-trajectories ending at the point of ACE-FTS measurement (49.14° N, 132.10° W) at 11.5 km. Trajectories are initialized from this location in 12 hour increments, with the latest start time occurring on July 30<sup>th</sup>, 2023 04:00 UTC (the time of measurement) and the earliest start time on July 26<sup>th</sup> 2023, 16:00 to compensate for limited ACE-FTS coverage. ¶

**Deleted:** Cross-referencing with an online crowdsourced py... [1]

**Deleted:** It is therefore plausible that this pyroCb is the sou... [2]

**Deleted:** <object>

**Deleted:** Yukon event

**Deleted:** 7

**Deleted:** plume

**Deleted:** exhibiting

**Deleted:** wildfire smoke up to 10 km

**Deleted:** the tropopause

**Deleted:** ~1 km injection height

**Deleted:** Yukon event.

**Formatted:** Font color: Text 1

**Deleted:** 7

**Deleted:** Yukon event measured by ss107570

**Deleted:** . The altitude is relative to the tropopause heig... [3]

**Moved down [4]:** (D'Angelo et al., 2022).

**Deleted:** <object>The maximum VMR and aerosol extinct... [4]

**Deleted:** 8

**Deleted:** between 11.5 and 16.5 km,

**Deleted:** and longer-lasting

**Deleted:** into the stratosphere

**Formatted:** Font color: Red

**Deleted:** 8

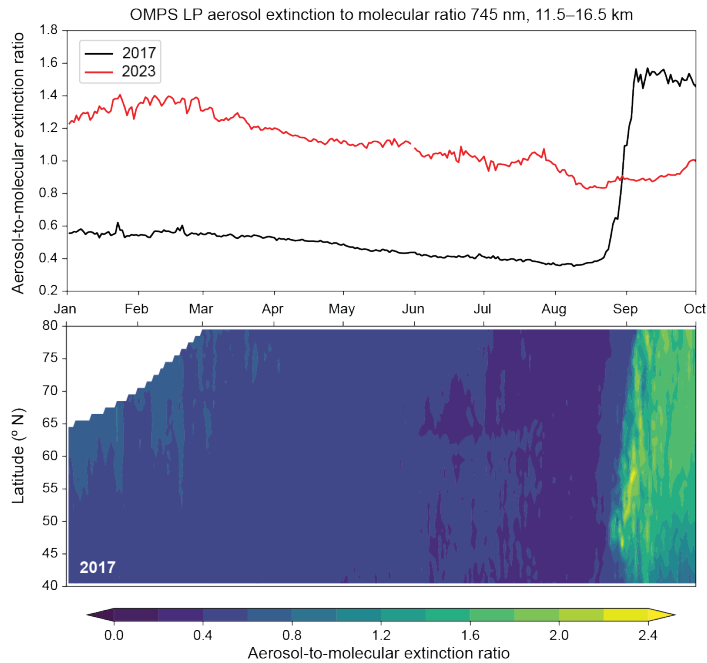
measured only a handful of occultations with stratospheric signatures of smoke and the OMPS LP aerosol data does not feature any significant perturbations in 2023 past 12 km, we conclude that the 2023 Canadian wildfire season did not significantly impact stratospheric composition relative to previous years despite burning a far larger area and exhibiting frequent pyroCb activity.

Deleted: one occultation

Deleted: clear

Deleted:

Formatted: Font: 9 pt, Bold, Font color: Auto



455 **Figure 7:** Top panel: average OMPS aerosol-to-molecular extinction ratio from 40 and 80° N, 11.5 to 16.5 km compared between 2017 (black) and 2023 (red). Bottom panel: 2017 zonally averaged OMPS extinction between 11.5 and 16.5 km, 40 to 80° N.

Deleted: 8

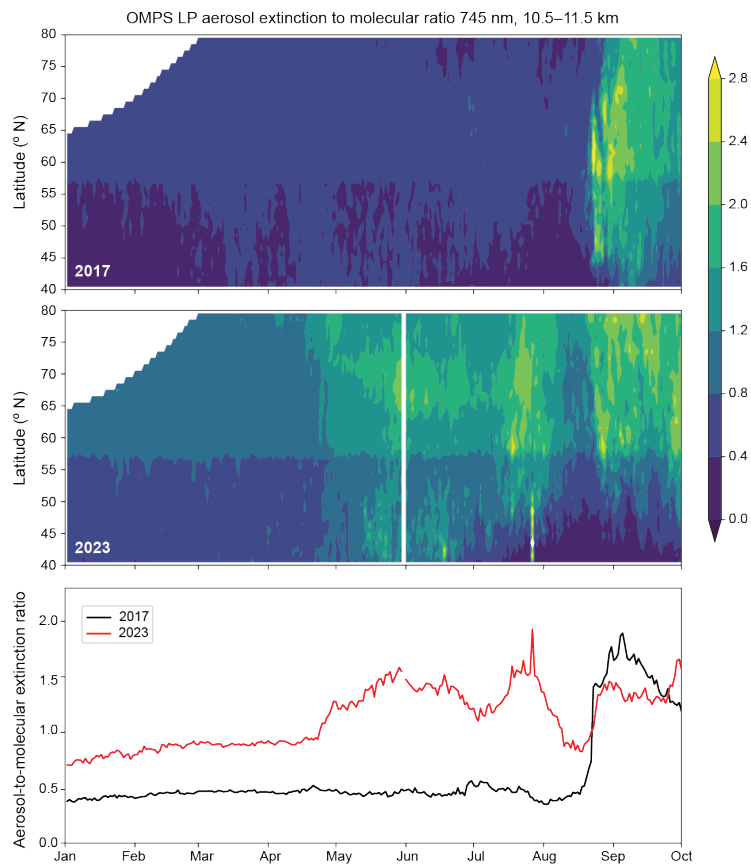
Formatted: Font: 9 pt, Bold

460 However, the aerosol loading near the tropopause is similar between the two years, as seen in Figure 8. It is clear that the active pyroCb activity in the 2023 wildfire season did influence upper tropospheric composition given the increase in aerosol extinction starting in May, which coincides with the start of the burning season. This is in stark contrast to the stratospheric aerosol loading from Figure 5, which is largest at the beginning of the year. Thus, the stratospheric PNE is visibly more significant since smoke following the event is measured well above the tropopause, whereas smoke from the 2023 fires remains around the tropopause throughout the entire wildfire season. This lower altitude of perturbation

corresponds to a shorter smoke lifetime in the stratosphere, further suggesting the lesser impact of the 2023 fires compared to the PNE (D'Angelo et al., 2022).

Moved (insertion) [4]

Formatted: Font color: Red



470

**Figure 8: Top panel: 2017 zonally averaged OMPS aerosol-to-molecular extinction ratio between 10.5 and 11.5 km, 40 to 80° N. Middle panel: 2023 zonally averaged OMPS aerosol-to-molecular extinction ratio between 10.5 and 11.5 km, 40 to 80° N. Bottom panel: average OMPS aerosol-to-molecular extinction ratio from 40 to 80° N, 10.5 to 11.5 km compared between 2017 (black) and 2023 (red).**

#### 475 4 Conclusions

Using ACE-FTS observations, we identified the presence of biomass burning products in the stratosphere in [a limited number of occultation measurements](#) over Canada during the 2023 summer wildfire season. This and ACE imager data, alongside OMPS LP aerosol data and MLS CO data, suggests that the immediate impacts of these fires are essentially limited to the troposphere, [with evidence only for nominal amounts of smoke in the lowermost stratosphere](#). Any aerosols that made it into the stratosphere remained near the tropopause and did not make it high enough to substantially influence stratospheric composition. However, carbonaceous aerosol has the potential to increase parcel buoyancy via solar heating and self-loft over longer timescales (de Laat et al., 2012; Yu et al., 2019; Ohneiser et al., 2023). The impacts of this process have not been pursued in this work but may have implications for climate and stratospheric composition. [Additionally, the climate implications of increased smoke in the upper troposphere is an active area of interest \(Christian et al., 2019; Kochaniski et al., 2019; Li et al., 2021\).](#)

In summary, this work shows that despite an extremely extensive wildfire season with frequent pyroCb activity in Canada, the conditions for sufficiently deep convection were met so rarely and to such a limited extent that no significant stratospheric perturbation took place. These results highlight that area alone is not a useful indicator of the potential for stratospheric effects, and projected increases in area burned per degree of global warming are not enough to forecast the vertical extents of future wildfires. The complexity of intense pyroCb formation motivates further study of why certain events, such as the 2019 – 2020 ANYSO and 2017 PNE, are more primed for stratospheric penetration. Factors including fire intensity and atmospheric structure may play an important role. Understanding which wildfire conditions enable stratospheric impacts, and how and where these may be realized under a changing climate, has significant implications for stratospheric ozone and climate.

#### Competing interests

The contact author has declared that none of the authors has any competing interests.

#### Acknowledgments

Selena Zhang was funded by the MIT John H. Olsen Presidential Fellowship. Susan Solomon gratefully acknowledges support by NSF-AGS grant 2316980. Funding for the Atmospheric Chemistry Experiment is provided by the Canadian Space Agency.

Deleted: only one

Deleted: measurement

Deleted: , and back and forward trajectories linked these elevated concentrations to a pyroCb event on July 24<sup>th</sup> in the Yukon....

Deleted: other

Deleted: constituent

Formatted: Font color: Red

Deleted: the

## References

510 Basha, G., Venkat Ratnam, M., and Kishore, P.: Asian summer monsoon anticyclone: trends and variability, *Atmos. Chem. Phys.*, 20, 6789-6801, <https://doi.org/10.5194/acp-20-6789-2020>, 2020.

Deleted: <https://doi.org/>

Bernath, P. F.: Atmospheric Chemistry Experiment (ACE): Mission Overview, Fourier Transform Spectroscopy/Hyperspectral Imaging and Sounding of the Environment, *JMA3*, <https://doi.org/10.1364/FTS.2005.JMA3>, 2005.

Deleted: <https://doi.org/>

515 Bernath, P. F.: The Atmospheric Chemistry Experiment (ACE), *J. Quant. Spectrosc. Ra.*, 186, 3-16, <https://doi.org/10.1016/j.jqsrt.2016.04.006>, 2017.

Bernath, P.: Vibrational Spectroscopy, in: *Spectra of Atoms and Molecules*, 4<sup>th</sup> Edition, Oxford University Press, Oxford, 260, 2020.

Bernath, P., Boone, C., and Crouse, J.: Wildfire Smoke Destroys Stratospheric Ozone, *Science*, 375, 1292-1295, <https://doi.org/10.1126/science.abm5611>, 2022.

Deleted: <https://doi.org/>

520 Boone, C. D., Bernath, P. F., and Fromm, M. D.: Pyrocumulonimbus Stratospheric Plume Injections Measured by the ACE-FTS, *Geophys. Res. Lett.*, 47, e2020GL088442, <https://doi.org/10.1029/2020GL088442>, 2020.

Boone, C. D., Bernath, P. F., and Lecours, M.: Version 5 Retrievals for ACE-FTS and ACE-Imagers, *J. Quant. Spectrosc. Ra.*, 310, 108749, <https://doi.org/10.1016/j.jqsrt.2023.108749>, 2023.

525 Boer, M. M., de Dios, R., and Bradstock, R. A.: Unprecedented burn area of Australian mega forest fires, *Nat. Clim. Change*, 10, 170-172, <https://doi.org/10.1038/s41558-020-0716-1>, 2020.

Deleted: <https://doi.org/>

Buijs, H. L., Soucy, M-A., and Lachance, R. L.: ACE-FTS Hardware and Level 1 Processing, in: *The Atmospheric Chemistry Experiment ACE at 10: A Solar Occultation Anthology*, edited by: Bernath, P. F., A. Deepak Publishing, Virginia, 53-80, 2013.

Canadian Interagency Forest Fire Centre Inc: Wildfire Graphs. <https://ciffc.net/statistics/>, last access: 10 January 2024.

530 Christian, K., Wang, J., Ge, C., Peterson, D., Hyer, E., Yorks, J., and McGill, M.: Radiative Forcing and Stratospheric Warming of Pyrocumulonimbus Smoke Aerosols: First Modeling Results With Multisensor (EPIC, CALIPSO, and CATS) Views from Space, *Geophys. Res. Lett.*, 46, 10061-10071, <https://doi.org/10.1029/2019GL082360>, 2019.

- D'Angelo, G., Guimond, S., Reisner, J., Peterson, D. A., and Dubey, M.: Contrasting Stratospheric Smoke Mass and Lifetime From 2017 Canadian and 2019/2020 Australian Megafires: Global Simulations and Satellite Observations, *J. Geophys. Res-Atmos.*, 127, e2021JD036249, <https://doi.org/10.1029/2021JD036249>, 2022.
- 540 Davey, S. M., and Sarre, A.: Editorial: the 2019/20 Black Summer bushfires, *Aust. For.*, 83, 47-51, <https://doi.org/10.1080/00049158.2020.1769899>, 2020.
- [De Laat, A. T. J., Stein Zweers, D. C., Boers, R., Tuinder, O. N. E., A solar escalator: Observational evidence of the self-lifting of smoke and aerosols by absorption of solar radiation in the February 2009 Australian Black Saturday plume, \*J. Geophys. Res-Atmos.\*, 117, D04204, <https://doi.org/10.1029/2011JD017016>, 2012.](#)
- 545 Di Virgilio, G., Evans, J. P., Blake, S. A., Armstrong, M., Dowdy, A. J., Sharples, J., and McRae, R.: Climate Change Increases the Potential for Extreme Wildfires, *Geophys. Res. Lett.*, 46, 8517-8526, <https://doi.org/10.1029/2019GL083699>, 2019.
- [Doeringer, D., Eldering, A., Boone, C. D., González Abad, G., Bernath, P. F.: Observation of sulfate aerosols and SO2 from the Sarychev volcanic eruption using data from the Atmospheric Chemistry Experiment \(ACE\). \*J. Geophys. Res-Atmos.\*, 117, <https://doi.org/10.1029/2011JD016556>, 2012.](#)
- 550 Fromm, M., Lindsey, D. T., Servranckx, R., Yue, G., Trickl, T., Sica, R., Doucet, P., and Godin-Beekmann, S.: The Untold Story of Pyrocumulonimbus, *B. Am. Meteorol. Soc.*, 91, 1193-1210, <https://doi.org/10.1175/2010BAMS3004.1>, 2010.
- Fromm, M., Peterson, D., and Di Girolamo, L.: The Primary Convective Pathway for Observed Wildfire Emissions in the Upper Troposphere and Lower Stratosphere: A Targeted Reinterpretation, *J. Geophys. Res.*, 124, 13254-13272, <https://doi.org/10.1029/2019JD031006>, 2019.
- 555 Fromm, M., Servranckx, R., Stocks, B. J., and Peterson, D. A.: Understanding the Critical Elements of the Pyrocumulonimbus Storm Sparked by High-Intensity Wildland Fire, *Commun. Earth Environ.*, 3, 243, <https://doi.org/10.1038/s43247-022-00566-8>, 2022.
- [Hersbach, H., Bell, B., Berrisford, P., Biavati, G., Horányi, A., Muñoz Sabater, J., Nicolas, J., Peubey, C., Radu, R., Rozum, I., Schepers, D., Simmons, A., Soci, C., Dee, D., and Thépaut, J.-N.: ERA5 hourly data on single levels from 1940 to present. Copernicus Climate Change Service \(C3S\) Climate Data Store \(CDS\), <https://doi.org/10.24381/cds.adbb2d47>, 2023.](#)
- 560

Deleted: https://doi.

Deleted: https://doi.

Deleted: de

Deleted: https://doi.

Deleted: https://doi.

Deleted: https://doi.

Deleted: https://doi.

Deleted: https://doi.

Formatted: Font color: Text 1

570 [Homeyer, C. R., Pan, L. L., Dorsi, S. W., Avallone, L. M., Weinheimer, A. J., O'Brien, A. S., DiGangi, J. P., Zondlo, M. A., Ryerson, T. B., Diskin, G. S., Campos, T. L., Convective transport of water vapor into the lower stratosphere observed during double-tropopause events, \*J. Geophys. Res. Atmos.\*, \*\*119\*\*, 10941-10958, <https://doi.org/10.1002/2014JD021485>, 2014.](#)

Kablick III, G. P., Allen, D. R., Fromm, M. D., and Nedoluha, G. E.: Australian PyroCb Smoke Generates Synoptic-Scale Stratospheric Anticyclones, *Geophys. Res. Lett.*, **47**, e2020GL088101, <https://doi.org/10.1029/2020GL088101>, 2020.

**Deleted:** <https://doi.org/10.1029/2020GL088101>,

575 Khaykin, S., Legras, B., Bucci, S., Sellitto, P., Isaksen, L., Tencé, F., Bekki, S., Bourassa, A., Rieger, L., Zawada, D., Jumelet, J., and Godin-Beekmann, S.: The 2019/20 Australian wildfires generated a persistent smoke-charged vortex rising up to 35km altitude, *Commun. Earth Environ.*, **1**, 22, <https://doi.org/10.1038/s43247-020-00022-5>, 2020.

**Deleted:** <https://doi.org/10.1038/s43247-020-00022-5>

[Kochanski, A. K., Mallia, D. V., Fearon, M. G., Mandel, J., Sourì, A. H., and Brown, T.: Modeling Wildfire Smoke Feedback Mechanisms Using a Coupled Fire-Atmosphere Model With a Radiatively Active Aerosol Scheme, \*J. Geophys. Res-Atmos.\*, \*\*124\*\*, 9099-9116, <https://doi.org/10.1029/2019JD030558>, 2019.](#)

580 [Lestrelin, H., Legras, B., Podglajen, A., and Salihoglu, M.: Smoke-charged vortices in the stratosphere generated by wildfires and their behaviour in both hemispheres: comparing Australia 2020 to Canada 2017, \*Atmos. Chem. Phys.\*, \*\*21\*\*, 7113-7134, <https://doi.org/10.5194/acp-21-7113-2021>, 2021.](#)

Li, Q., Jacob, D. J., Bey, I., Yantosca, R. M., Zhao, Y., Kondo, Y., Notholt, J.: Atmospheric Hydrogen Cynaide (HCN): Biomass Burning Source, Ocean Sink?, *Geophys. Res. Lett.*, **27**, 357-360, <https://doi:10.1029/1999gl010935>, 2000.

[Li, Y., Dykema, J., Deshler, T., and Keutsch, F.: Composition Dependence of Stratospheric Aerosol Shortwave Radiative Forcing in Northern Midlatitudes, \*Geophys. Res. Lett.\*, \*\*48\*\*, e2021GL094427, <https://doi.org/10.1029/2021GL094427>, 2021.](#)

590 Livesey, N. J., Read, W. G., Wagner, P. A., Froidevaux, L., Santee, M. L., Schwartz, M. J., Lambert, A., Valle, L. F. M., Pumphrey, H. C., Manney, G. L., Fuller, R. A., Jarnot, R. F., Knosp, B. W., and Lay, R. R.: Version 5.0x Level 2 and 3 data quality and description document, Tech. Rep. JPL D-105336 Rev. B, Jet Propulsion Laboratory, California Institute of Technology, Pasadena, California, [https://mls.jpl.nasa.gov/data/v5-0\\_data\\_quality\\_document.pdf](https://mls.jpl.nasa.gov/data/v5-0_data_quality_document.pdf) (last access: 21 Jan 2024), 2022.

**Deleted:** <https://mls>.

595 [Loughman, R., Bhartia, P. K., Chen, Z., Xu, P., Nyaku, E., and Taha, G.: The Ozone Mapping and Profiler Suite \(OMPS\) Limb Profiler \(LP\) Version 1 aerosol extinction retrieval algorithm: theoretical basis, \*Atmos. Meas. Tech.\*, \*\*11\*\*, 2633-2651, <https://doi.org/10.5194/amt-11-2633-2018>, 2018.](#)



MODIS Moderate Resolution Imaging Spectroradiometer: July 5, 2023 – Fire and Smoke in Russia’s Far East.  
600 [https://modis.gsfc.nasa.gov/gallery/individual.php?db\\_date=2023-07-05](https://modis.gsfc.nasa.gov/gallery/individual.php?db_date=2023-07-05), last access: 27 February 2024.

[Ohneiser, K., Ansmann, A., Witthuhn, J., Deneke, H., Chudnovsky, A., Walter, G., and Senf, F.: Self-lofting of wildfire smoke in the troposphere and stratosphere: simulations and space lidar observations, Atmos. Chem. Phys., 23, 2901-2925, <https://doi.org/10.5194/acp-23-2901-2023>, 2023.](#)

Pausas, J. G. and Keeley, J. E.: Wildfires and Global Change, Front. Ecol. Environ., 19, 387-395,  
605 <https://doi.org/10.1002/fee.2359>, 2021.

[Peevey, T. R., Gille, J. C., Randall, C. E., and Kunz, A.: Investigation of double tropopause spatial and temporal global variability utilizing High Resolution Dynamics Limb Sounder temperature observations, J. Geophys. Res. Atmos., 117, D1, <https://doi.org/10.1029/2011JD016443>, 2012.](#)

Peterson, D. A., Hyer, E. J., Campbell, J. R., Solbrig, J. E., and Fromm, M. D.: A Conceptual Model for Development of  
610 Intense Pyrocumulonimbus in Western North America, Mon. Weather Rev., 145, 2235-2255, <https://doi.org/10.1175/MWR-D-16-0232.1>, 2017.

Peterson, D. A., Campbell, J. R., Hyer, E. J., Fromm, M. D., Kablick III, G. P., Cossuth, J. H., and Deland, M. T.: Wildfire-driven thunderstorms cause a volcano-like stratospheric injection of smoke, npj Clim. Atmos. Sci., 1, 30,  
<https://doi.org/10.1038/s41612-018-0039-3>, 2018.

615 Peterson, D. A., Fromm, M. D., McRae, R. H. D., Campbell, J. R., Hyer, E. J., Taha, G., Camacho, C. P., Kablick III, G. P., Schmidt, C. C., and DeLand, M. T.: Australia’s Black Summer pyrocumulonimbus super outbreak reveals potential for increasingly extreme stratospheric smoke events, npj Clim. Atmos. Sci., 4, 38, <https://doi.org/10.1038/s41612-021-00192-9>, 2021.

620 [Renard, J-B., Berthet, G., Levasseur-Regourd, A-C., Beresnev, S., Miffre, A., Rairoux, P., Vignelles, D., Jégou, F.: Origins and Spatial Distribution of Non-Pure Sulfate Particles \(NSPs\) in the Stratosphere Detected by the Balloon-Borne Light Optical Aerosols Counter \(LOAC\), Atmosphere, 11, 1031, <https://doi.org/10.3390/atmos11101031>, 2020.](#)

Rieger, L. A., Randel, W. J., Bourassa, A. E., and Solomon, S.: Stratospheric Temperature and Ozone Anomalies Associated With the 2020 Australian New Year Fires, Geophys. Res. Lett., 48, e2021GL095898,  
<https://doi.org/10.1029/2021GL095898>, 2021.

**Moved down [5]:** Data Chat: Dr. David Peterson.  
<https://www.earthdata.nasa.gov/learn/data-chats/david-peterson>, last access: 3 February 2024.

**Deleted:** NASA EarthData:

**Deleted:** ¶

**Formatted:** Font color: Auto

**Deleted:** <https://doi>.

**Deleted:** <https://doi>.

**Deleted:** <https://doi>.

635 Roberts, J. M., Stockwell, C. E., Yokelson, R. J., de Gouw, J., Liu, Y., Selimovic, V., Koss, A. R., Sekimoto, K., Coggon,  
M. M., Yuan, B., Zarzana, K. J., Brown, S. S., Santin, C., Doerr, S. H., and Warneke, C.: The nitrogen budget of laboratory-  
simulated western US wildfires during the FIREX 2016 Fire Lab study, *Atmos. Chem. Phys.*, 20, 8807-8826,  
<https://doi.org/10.5194/acp-20-8807-2020>, 2020.

Romps, D. M., and Kuang, Z.: Overshooting convection in tropical cyclones, *Geophys. Res. Lett.*, 36, L09804,  
<https://doi.org/10.1029/2009GL037396>, 2009.

640 [Sica, R. J., Izawa, M. R. M., Walker, K. A., Boone, C., Petelina, S. V., Argall, P. S., Bernath, P., Burns, G. B., Catoire, V.,  
Collins, R. L., Daffer, W. H., De Clercq, C., Fan, Z. Y., Firanski, B. J., French, W. J. R., Gerard, P., Gerding, M., Granville,  
J., Innis, J. L., Keckhut, P., Kerzenmacher, T., Klekociuk, A. R., Kyrö, E., Lambert, J. C., Llewellyn, E. J., Manney, G. L.,  
McDermid, I. S., Mizutani, K., Murayama, Y., Piccolo, C., Raspollini, P., Ridolfi, M., Robert, C., Steinbrecht, W.,  
Strawbridge, K. B., Strong, K., Stubi, R., and Thurairajah, B.: Validation of the Atmospheric Chemistry Experiment \(ACE\)  
version 2.2 temperature using ground-based and space-borne measurements, \*Atmos. Chem. Phys.\*, 8, 35-62,  
645 <https://doi.org/10.5194/acp-8-35-2008>, 2008.](#)

[Sellitto, P., Belhadji, R., Cuesta, J., Podglajen, A., & Legras, Bernard.: Radiative impacts of the Australian bushfires 2019-  
2020 – Part 2: Large-scale and in-vortex radiative heating, \*Atmos. Chem. Phys.\*, 23, 15523-15535,  
<https://doi.org/10.5194/acp-23-15523-2023>, 2023.](#)

650 [Smith, J. M.: Data Chat: Dr. David Peterson. <https://www.earthdata.nasa.gov/learn/data-chats/david-peterson>, last access: 3  
February 2024, 2023.](#)

Solomon, S., Stone, K., Yu, P., Murphy, D. M., Kinnison, D., Ravishankara, A. R., and Wang, P.: Chlorine activation and  
enhanced ozone depletion induced by wildfire aerosol, *Nature*, 615, 259-264, <https://doi.org/10.1038/s41586-022-05683-0>,  
2023.

655 Stein, A. F., Draxler, R. R., Rolph, G. D., Stunder, B. J. B., Cohen, M. D., and Ngan, F.: NOAA's HYSPLIT Atmospheric  
Transport and Dispersion Modeling System, *B. Am. Meteorol. Soc.*, 96, 2059-2077, [https://doi.org/10.1175/BAMS-D-14-  
00110.1](https://doi.org/10.1175/BAMS-D-14-<br/>00110.1), 2015.

Taha, G., Loughman, R., Zhu, T., Thomason, L., Kar, J., Rieger, L., and Bourassa, A.: OMPs LP Version 2.0 Multi-  
Wavelength Aerosol Extinction Coefficient Retrieval Algorithm, *Atmos. Meas. Tech.*, 14, 1015-1036,  
<https://doi.org/10.5194/amt-14-1015-2021>, 2021.

Formatted: Font: +Body (Times New Roman)

Moved (insertion) [5]

Formatted: Font: 10 pt, Font color: Auto

Formatted: Font: 10 pt

Formatted: Font: 10 pt

Formatted: Font: 10 pt

Formatted: Font: 10 pt

Formatted: Font: +Body (Times New Roman)

Formatted: Font: +Body (Times New Roman), Not Bold

660 [Taha, G., Loughman, R., Colarco, P. R., Zhu, T., Thomason, L. W., and Jaross, G.: Tracking the 2022 Hunga Tonga-Hunga Ha'apai Aerosol Cloud in the Upper and Middle Stratosphere Using Space-Based Observations, \*Geophys. Res. Lett.\*, \*\*49\*\*, e2022GL100091, <https://doi.org/10.1029/2022GL100091>, 2022.](#)

Thurston, G., Yu, W., and Luglio, D.: An Evaluation of the Asthma Impact of the June 2023 New York City Wildfire Air Pollution Episode, *Am. J. Resp. Crit. Care*, 208, 898-900, <https://doi.org/10.1164/rccm.202306-1073LE>, 2023.

665 [Torres, O., Bhartia, P. K., Taha, G., Jethva, H., Das, S., Colarco, P., Krotkov, N., Omar, A., and Ahn, C.: Stratospheric Injection of Massive Smoke Plume From Canadian Boreal Fires in 2017 as Seen by DSCOVR-EPIC, CALIOP, and OMPS-LP Observations, \*J. Geophys. Res-Atmos.\*, \*\*125\*\*, e2020JD032579, <https://doi.org/10.1029/2020JD032579>, 2020.](#)

670 [Vanhellemont, F., Tetard, C., Bourassa, A., Fromm, M., Dodion, J., Brogniez, C., Degenstein, D., Gilbert, K. L., Turnbull, D. N., Bernath, P., Boone, C., and Walker, K. A.: Aerosol extinction profiles at 525 nm and 1020 nm derived from ACE imager data: comparisons with GOMOS, SAGE II, SAGE III, POAM III, and OSIRIS, \*Atmos. Chem. Phys.\*, \*\*8\*\*, 2027-2037, <https://doi.org/10.5194/acp-8-2027-2008>, 2008.](#)

Wang, Z., Wang, Z., Zou, Z., Chen, X., Wu, H., Wang, W., Su, H., Li, F., Xu, W., Liu, Z., and Zhu, J.: Severe Global Environmental Issues Caused by Canada's Record-Breaking Wildfires in 2023, *Adv. Atmos. Sci.*, <https://doi.org/10.1007/s00376-023-3241-0>, 2023.

675 [Waters, J., Froidevaux, L., Harwood, R., Jarnot, R., Pickett, H., Read, W., Siegel, P., Cofield, R., Filipiak, M., Flower, D., Holden, J., Lau, G., Livesey, N., Manney, G., Pumphrey, H., Santee, M., Wu, D., Cuddy, D., Lay, R., Loo, M., Perun, V., Schwartz, M., Stek, P., Thurstans, R., Boyles, M., Chandra, K., Chavez, M., Chen, G.-S., Chudasama, B., Dodge, R., Fuller, R., Girard, M., Jiang, J., Jiang, Y., Knosp, B., LaBelle, R., Lam, J., Lee, K., Miller, D., Oswald, J., Patel, N., Pukala, D., Quintero, O., Scaff, D., Van Snyder, W., Tope, M., Wagner, P., and Walch, M.: The earth observing system microwave limb sounder \(EOS MLS\) on the Aura satellite, \*IEEE T. Geosci. Remote\*, \*\*44\*\*, 1075–1092, <https://doi.org/10.1109/TGRS.2006.873771>, 2006.](#)

680 [Williams, A. P., Abatzoglou, J. T., Gershunov, A., Guzman-Morales, J., Bishop, D. A., Balch, J. K., and Lettenmaier, D. P.: Observed Impacts of Anthropogenic Climate Change on Wildfire in California, \*Earth's Future\*, \*\*7\*\*, 892-910, <https://doi.org/10.1029/2019EF001210>, 2019.](#)

685 [World Meteorological Organization: Meteorology—A three-dimensional science: Second session of the commission for aerology, \*WMO Bull.\*, \*\*4\*\*, 134–138, 1957.](#)

Deleted:

Formatted: Font color: Auto, Pattern: Clear

690

Xiao, Y., Jacob, D. J., Wang, J. S., Logan, J. A., Palmer, P. I., Suntharalingam, P., Yantosca, R. M., Sachse, G. W., Blake, D. R., Streets, D. G.: Constraints on Asian and European sources of methane from CH<sub>4</sub>-C<sub>2</sub>H<sub>6</sub>-CO correlations in Asian outflow, *J. Geophys. Res-Atmos.*, 109, D15S16, <https://doi.org/10.1029/2003JD004475>, 2004.

Yu, P., Toon, O. B., Bardeen, C. G., Zhu, Y., Rosenlof, K. H., Portmann, R. W., Thornberry, T. D., Gao, R-S., Davis, S. M., Wolf, E. T., de Gouw, J., Peterson, D. A., Fromm, M. D., and Robock, A.: Black carbon lofted wildfire smoke high into the stratosphere to form a persistent plume, *Science*, 365, 587-590, <https://doi.org/10.1126/science.aax1748>, 2019.

Zhong, M., and Jang, M.: Dynamic light absorption of biomass-burning organic carbon photochemically aged under natural sunlight, *Atmos. Chem. Phys.*, 14, 1517-1525, <https://doi.org/10.5194/acp-14-1517-2014>, 2014.

Deleted:

**Page 10: [1] Deleted      Selena Zhang      8/27/24 6:40:00 PM**



**Page 10: [2] Deleted      Selena Zhang      8/27/24 6:40:00 PM**



**Page 10: [3] Deleted      Selena Zhang      8/27/24 6:40:00 PM**



**Page 10: [4] Deleted      Selena Zhang      8/27/24 6:40:00 PM**

